Journal of Molecular Liquids xxx (2020) xxx

Contents lists available at ScienceDirect

Journal of Molecular Liquids

journal homepage: www.elsevier.com/locate/molliq

Introduction of isothiuronium surfactant series: Synthesis, structure-dependent aggregation overview and biological activity

F.G. Valeeva [a], T.R. Karimova [a], R.V. Pavlov [a], D.I. Bakhtiyarov [b], A.S. Sapunova [a], K.A. Ivshin [a], O.N. Kataeva [a], G.A. Gaynanova [a,*], V.V. Syakaev [a], A.D. Voloshina [a], I.V. Galkina [b], Sh.K. Latypov [a], L.Ya. Zakharova [a]

[a] Arbuzov Institute of Organic and Physical Chemistry, FRC Kazan Scientific Center of RAS, 8 Arbuzov str., 420088, Kazan, Russian Federation
[b] Kazan Federal University, 18 Kremlyovskaya str., 420008 Kazan, Russian Federation

ARTICLE INFO

Article history:
Received 23 July 2020
Received in revised form 1 November 2020
Accepted 5 November 2020
Available online xxxx

Keywords:
Isothiuronium cationic surfactant
Synthesis
Self-assembly
Solubilization
Aggregation number

ABSTRACT

For a homologous series of isothiuronium surfactants (S-alkylisothiuronium bromides, C_nSU, where $n = 10, 12, 14, 16, 18$), a synthesis procedure is described and aggregation properties are comprehensively characterized by a variety of techniques. Krafft temperature and critical micelle concentration (cmc) are obtained by methods of conductometry, tensiometry, spectrophotometry, fluorimetry. Using dynamic light scattering and NMR diffusometry, aggregate sizes in aqueous solutions were determined. The aggregation numbers of C_nSU systems were estimated by alternative methods. An increase in the length of the alkyl tail from 10 to 16 carbon atoms leads to a decrease in cmc from 16 to 0.5 mM with a decrease in aggregation numbers. S-alkylisothiuronium bromides exhibit solubilization capacity toward a hydrophobic dye Orange OT which is 2–3 times higher than that of alkyltrimethylammonium analogues. Improved solubilization characteristics along with antimicrobial properties manifested at the concentrations of low hemolytic activity allow us to recommend these amphiphiles for the fabrication of soft nanocontainers for hydrophobic guests showing their own biological functionality.

© 2020 Elsevier B.V. All rights reserved.

1. Introduction

Surfactants practical applications, such as nanoparticle synthesis, micellar catalysis, emulsion polymerization, solubilization of biologically active and medicinal substances, detergent industry and oil production, are based on their ability to reduce surface tension, form nanoscale aggregates and influence wettability [1–8]. Cationic surfactants have a special place among the others [2,9,10], since interest in them is growing quickly due to applications in cosmetics and pharmaceutics [11], corrosion inhibition [12] and nanomaterial synthesis [13]. The synthesis of new amphiphilic compounds with the introduction of functional fragments into the head group or the replacement of a charge-bearing atom is a worldwide practice in the search for new nanocontainers, nanoreactors, antimicrobial compositions based on surfactants. The bulk of the experimental material in this direction was obtained by the example of ammonium salts. A new generation of surfactants should, along with the preserved properties, have less toxicity to living organisms [14,15]. One of the trends in reducing toxicity is the transition to gemini surfactants, since they are characterized by very low critical micelle concentration (cmc) values, which allows working with them in the micro- and millimolar concentration ranges [16]. They are of increasing popularity in many fields of study [17]. But sometimes such surfactants have a high production cost due to synthesis aspects. Another trend is application of biodegradable surfactants [14,18]. Researchers implement biodegradable parts such as aminoacid, carbamate, amide or ester groups to lower ecological aftermath [19–23].

Compounds with an isothiuronium fragment attracted our attention, since this functional group has a number of practically useful properties, including antibacterial [24–26], catalytic [27,28], antituberculosis [29] activities, and also plays an important role in many chemical and biological processes, for example, they have been explored as an agonists of GABA-type receptors [30], short-chain (<C4) S-alkylisothioureas can be considered to be prodrugs of the aldehyde dehydrogenase inhibitor cyanamide [31]. It is known that the isothiuronium group sewn to the surface of halloysite is able to extract uranium [32] from aqueous solutions, and polystyrene – divinylbenzene resins functionalized with isothiouronium allows efficient binding of palladium from acidic solutions [33]. A series of aryl- and alkyl-substituted isothiuronium salts was synthesized in [34] and it was shown that alkyl substituents exhibit high anticancer activity and selectivity for leukemia cells.

In the large volume of articles devoted to the synthesis and study of the properties of isothiuronium salts, only a few describe the properties of amphiphilic derivatives [26,35–38]. Based on the series of azobenzene isothiouronium salts of different alkyl chains (propyl, hexyl and dodecyl), metal complexes were obtained, their surface-

* Corresponding author.
E-mail address: ggulnara@bk.ru (G.A. Gaynanova).

https://doi.org/10.1016/j.molliq.2020.114721
0167-7322/© 2020 Elsevier B.V. All rights reserved.

Please cite this article as: F.G. Valeeva, T.R. Karimova, R.V. Pavlov, et al., Introduction of isothiuronium surfactant series: Synthesis, structure-dependent aggregation overview..., Journal of Molecular Liquids, https://doi.org/10.1016/j.molliq.2020.114721

active properties and biological activity toward the pathogenic Gram-negative bacteria, Gram-positive bacteria, and fungi [26]. The results indicate that the copper complexes of the synthesized azobenzene isothiouronium salts have a relatively higher biocidal activity than the parent salts.

The authors of [35] synthesized a number of new cationic surfactants, isothiuroniumethylalkyldimethylammonium bromides, which contain split hydrophilic isothiouronium head groups covalently attached to tertiary amines with alkyl chain of C_8-C_{12}. These surfactants have high cmc values from 300 mM for C_8 and up to 10 mM for C_{12}, which allows them to compact plasmid DNA. A practically useful property of the isothiouronium group is that it can be hydrolyzed to form a sulfhydryl group at pH above 8.5 and a temperature closer to 333 K. As a result of hydrolysis, surfactants with a lower cmc value are formed, and the thiol group can undergo further reaction after surfactant accumulation on the DNA matrix to form a lipid containing a disulfide bond and two alkyl chains. Template self-assembly of vesicles from a single-tailed surfactant isothiuroniumethylhexadecyldimethylammonium bromide followed by dimerization of surfactant molecules was described [36]. This leads to additional stability of nanocontainers under changing environmental conditions (pH, temperature, salt concentration).

The surface properties of the cationic surfactant dodecyl isothiouronium bromide in a mixed solvent of water and polyethylene glycol with different molecular weights (ethylene glycol, triethylene glycol and polyethylene glycol-600) are described in [37]. By the methods of tensiometry and conductometry, it was established that an increase in the molecular weight of glycols leads to an increase in the cmc value, and an increase in the mass fraction of glycol in the mixed solution, on the contrary, decreases the cmc value.

The surface properties of polyvinyl alcohol and three synthesized cationic surfactants were studied, namely S-dodecyl-, S-tetradecyl-, and S-hexadecyl isothiouronium bromide surfactant [38]. The cmc value for the dodecyl derivative is 4.2 mM, for tetradecyl - 1.95 mM, for hexadecyl - 0.58 mM in an individual aqueous solution. The formation of a mixed polymer compositions with an isothiouronium surfactant at molar ratios of 1:9, 3:7, 5:5, 7:3, and 9:1 lead to an increase in cmc values. It is important to note that all studies were carried out in aqueous solutions at 25°C, and the cmc values were determined by only one method — the measurement of surface tension by the ring detachment method.

Taking into account all of the above, the aim of this work was to synthesize a number of S-alkylisothiuronium bromides (C_nSU) (Fig. 1, where $n = 10, 12, 14, 16, 18$) according to the original procedure and to prove the exact structure of the obtained compounds using the methods of IR-, ^1H and ^{13}C NMR spectroscopy, x-ray structural analysis. Then planned to study their self-assembly in an aqueous solution by a complex of physicochemical methods (tensiometry, conductometry, spectrophotometry, dynamic and electrophoretic light scattering, fluorimetry, NMR) to obtain comprehensive information about nanocontainers based on relatively new types of surfactants with an assessment of their biological activity as well.

2. Materials and methods

2.1. Chemicals

Fluorescent probe pyrene (≥99%, Sigma Aldrich), hydrophobic dye Orange OT (75%, Sigma Aldrich), cetylpyridinium bromide (99%, AppliChem) were used as received. Purified water (18.2 MΩ cm resistivity at 25 °C) from Direct-Q 5 UV equipment was used for all solution preparation.

2.2. General synthesis procedure of S-n-alkylisothiuronium bromides

Firstly, synthesis of S-alkylisothiuronium salts (dodecyl, hexadecyl and octadecyl derivatives) was described in [39] without specifying the structural formula of the obtained salts. Our group planned to synthesize the whole range of compounds starting with a decyl derivative, the procedure was modified as follows. A solution of 1.0 g (0.01314 mol) of thiourea in 25 mL of ethyl alcohol with a small addition of diethyl ether (9:1) was heated in a water bath until the crystals of thiourea were completely dissolved. Equimolar amount of alkyl bromide was then added dropwise with stirring. The reaction mixture was heated in a flask under reflux for an appropriate time, which is listed for each compound separately, at a temperature of 78 °C. After completion of the reaction, a white precipitate formed upon cooling the reaction mixture. The precipitate was dried on a rotary evaporator and recrystallized - dissolved in acetone and precipitated by diethyl ether. The white precipitate was dried in vacuo. The structures of surfactants were confirmed by elemental analysis, IR (Spectrum Two FT-IR spectrometer) and ^1H and ^{13}C NMR spectroscopy. IR and NMR spectra are given in SI (Figs. S1-S5).

2.3. Characterization of S-n-alkylisothiuronium bromides

2.3.1. S-n-decylisothiuronium bromide ($C_{10}SU$)

Reflux time: 5 h. Yield: 91%, melt. = 103.6°C. Decomp. 226.7°C. M.w. 279.30.

Elem. anal. Found: % C, 44.23; H, 8.67; N, 9.30; S, 10.69. $C_{11}H_{25}BrN_2S$ calc. %: C, 44.44; H, 8.48; N, 9.42; S, 10.79. IR, ν, cm^{-1}: 3300–3000 (NH), 2918–2850 (CH), 1649 (C=N). ^1H NMR ($CDCl_3$, 500 MHz, δ, ppm, J, Hz): 0.892 (t, $^3J_{HH} = 7.1$ Hz, 3H, CH_3), 1.20–1.50 (m, 14H, $(CH_2)_7$), 1.75 (m, 2H, CH_2), 3.32 (t, $^3J_{HH} = 7.2$ Hz, 2H, CH_2S), 7.95 (br, 2H, NH_2), 9.26 (br, 2H, NH_2). $^{13}C\{H\}$ NMR ($CDCl_3$, 126 MHz, δ, ppm): 172.7 (C1), 32.4 (C2), 32.0–22.9 (C4-C9), 28.6 (C3), 14.3 (C10).

2.3.2. S-n-dodecylisothiuronium bromide ($C_{12}SU$)

Reflux time: 6 h. Yield: 87%, melt. = 109.5°C. Decomp. 225°C. M.w. 327.35.

Elem. anal. Found: % C, 47.79; H, 8.81; N, 8.31; S, 9.98. $C_{13}H_{29}BrN_2S$ calc. %: C, 47.99; H, 8.98; N, 8.61; S, 9.86. IR, ν, cm^{-1}: 3300–3000 (NH), 2912–2848 (CH), 1625 (C=N). ^1H NMR ($CDCl_3$, 500 MHz): 0.892 (t, $^3J_{HH} = 7.1$ Hz, 3H, CH_3), 1.20–1.50 (m, 18H, $(CH_2)_9$), 1.738

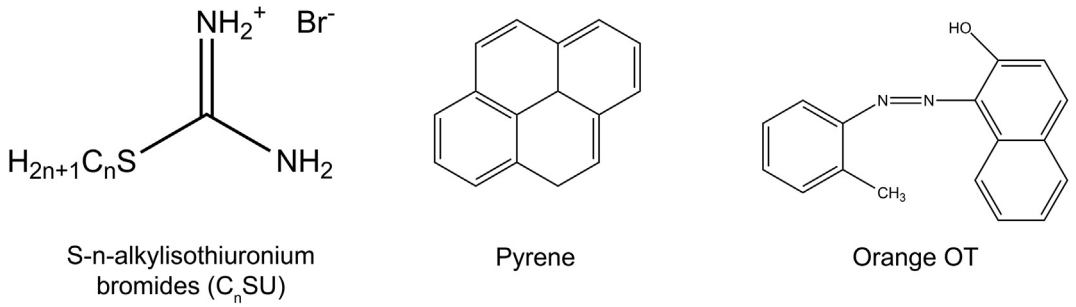

Fig. 1. Chemical formulas of compounds used in the work.

(m, 2H, CH_2), 3.294 (t, $^3J_{HH}$ = 7.2 Hz, 2H, CH_2S), 7.659 (br, 2H, NH_2), 9.265 (br, 2H, NH_2). $^{13}C\{H\}$ NMR ($CDCl_3$, 126 MHz, δ, ppm): 172.7 (C1), 32.3 (C2), 32.1–22.9 (C4-C11), 28.4 (C3), 14.3 (C12). ^{15}N NMR ($CDCl_3$, 51 MHz, δ, ppm): 109.1 (N1,N3).

2.3.3. S-n-tetradecylisothiuronium bromide ($C_{14}SU$)

Reflux time: 7 h. Yield: 92%, melt. = 113.2°C. Decomp. 225°C. M.w. 353.40.

Elem. anal. Found: % C, 50.78; H, 9.62; N, 7.61; S, 9.25. $C_{15}H_{33}BrN_2S$ calc. %: C, 50.98; H, 9.41; N, 7.93; S, 9.07. IR, ν, cm^{-1}: 3300–3000 (NH), 2915–2847 (CH), 1649 (C=N). ^1H NMR ($CDCl_3$, 500 MHz): 0.89 (t, $^3J_{HH}$ = 7.1 Hz, 3H, CH_3), 1.20–1.50 (m, 14H, $(CH_2)_{11}$), 1.78 (m, 2H, CH_2), 3.32 (t, $^3J_{HH}$ = 7.2 Hz, 2H, CH_2S), 7.48 (br, 2H, NH_2), 9.30 (br, 2H, NH_2). $^{13}C\{H\}$ NMR ($CDCl_3$, 126 MHz, δ, ppm): 172.8 (C1), 32.5 (C2), 32.1–22.9 (C4-C13), 28.7 (C3), 14.3 (C14).

2.3.4. S-n-hexadecylisothiuronium bromide ($C_{16}SU$)

Reflux time: 8 h. Yield: 88%, melt = 114.7°C. Decomp. 222.3°C. M.w. 381.46.

Elem. anal. found: % C, 53.40; H, 9.49; N, 7.15; S, 8.67. $C_{17}H_{37}BrN_2S$ calc. %: C, 53.53; H, 9.78; N, 7.34; S, 8.41. IR, ν, cm^{-1}: 3300–3000 (NH), 2915–2848 (CH), 1648 (C=N). ^1H NMR ($CDCl_3$, 500 MHz): 0.90 (t, $^3J_{HH}$ = 7.1 Hz, 3H, CH_3), 1.20–1.50 (m, 14H, $(CH_2)_{13}$), 1.78 (m, 2H, CH_2), 3.31 (t, $^3J_{HH}$ = 7.2 Hz, 2H, CH_2S), 7.36 (br, 2H, NH_2), 9.45 (br, 2H, NH_2). $^{13}C\{H\}$ NMR ($CDCl_3$, 126 MHz, δ, ppm): 172.9 (C1), 32.5 (C2), 32.1–22.9 (C4-C15), 28.6 (C3), 14.3 (C16).

2.3.5. S-n-octadecylisothiuronium bromide ($C_{18}SU$)

Reflux time: 9 h. Melt. 116.3°C. Decomp. 219.7°C. M.w. 409.51.

Elem. anal. found, % C, 53.55; H, 10.31; N, 6.60; S, 7.70. $C_{19}H_{41}BrN_2S$ calc. %: C, 53.73; H, 10.09; N, 6.84; S, 7.83. IR (KBr), ν, cm^{-1}: 3300–3000 (NH), 2915–2847 (CH), 1649 (C=N). ^1H NMR ($CDCl_3$, 500 MHz): 0.90 (t, $^3J_{HH}$ = 7.1 Hz, 3H, CH_3), 1.20–1.50 (m, 30H, $(CH_2)_{15}$), 1.67 (m, 2H, CH_2), 3.74 (t, $^3J_{HH}$ = 7.2 Hz, 2H, CH_2S), 7.01 (br, 2H, NH_2), 9.72 (br, 2H, NH_2). $^{13}C\{H\}$ NMR ($CDCl_3$, 126 MHz, δ, ppm): 172.0 (C1), 31.6 (C2), 31.5–22.3 (C4-C17), 28.1 (C3), 13.7 (C18).

2.3.6. X-ray crystallography

We managed to take a single crystal x-ray, but only for S-decylisothiuronium chloride, which was synthesized analogously to the bromide using decyl chloride. X-ray structural analysis data of the isothiuronium salts synthesized is shown in Fig. 2.

Data set for single crystal $C_{16}H_{45}ClN_{12}S_6$ was collected on a Bruker AXS Kappa APEX II CCD diffractometer with graphite-monochromated Mo Kα radiation (λ = 0.71073 Å). The structure was solved by direct methods using APEX3 for data collection, SAINT for data reduction, SHELXT [40] for structure solution, SHELXL [40] for structure refinement by full-matrix least-squares against F^2, and SADABS [41] for multi-scan absorption correction. Hydrogen atoms at carbon atoms were placed into calculated positions and refined as riding atoms. Hydrogen atoms at nitrogen atoms were revealed from difference Fourier map and refined isotropically with geometry constraints. Alkyl group is disordered. CCDC 2041059 contains the supplementary crystallographic data for this paper.

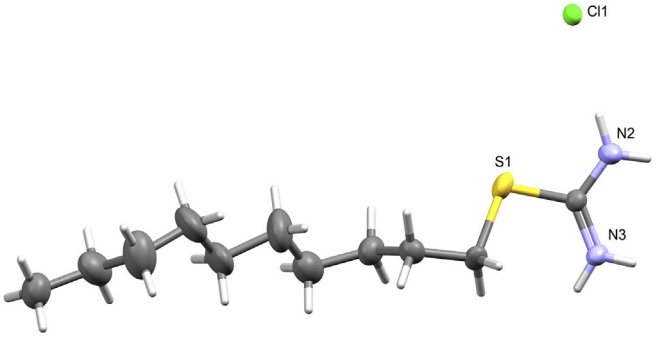

Fig. 2. S-decylisothiuronium chloride structure obtained from X-ray data.

Crystal data: formula $C_{16}H_{45}ClN_{12}S_6$, M = 633.45 g/mol, monoclinic, space group $P2_1/c$ (No. 14), $Z = 4$, $a = 24.956(2)$ Å, $b = 8.4210(7)$ Å, $c = 15.7289(13)$ Å, $\beta = 96.517(4)°$, $V = 3284.1(5)$ Å^3, $\rho_{calc} = 1.281$ g cm^{-3}, $\mu = 0.526$ mm^{-1}, 68,603 reflections collected ($-33 \le h \le 32$, $-11 \le k \le 11$, $-20 \le l \le 20$), θ range = 2.554° to 28.430°, 8241 independent ($R_{int} = 0.1299$) and 4667 observed reflections [$I \ge 2\sigma(I)$], 439 refined parameters, $R = 0.0589$, $wR^2 = 0.1424$, max.(min.) residual electron density 0.846 (−0.845) e Å^{-3}.

2.3.7. Thermogravimetry and differential scanning calorimetry

Melting and decomposition temperatures were studied by simultaneous thermogravimetry and differential scanning calorimetry thermoanalyzer STA 449C Jupiter (Netzsch) coupled with quadrupolar mass spectrometer QMS 403C Aeolos in the temperature range of 40–500 °C (Fig. S6). The heating rate was linear at 10°C/min. Approximately 10 mg of the compound was analyzed in an aluminum crucible in dynamic argon atmosphere with flowrate of 75 mL/min.

2.4. Surface tension measurement

The surface tension was measured using the Du Nouy ring detachment method on a K6 tensiometer (Kruss, Germany) with use of an optimally wettable platinum ring. The measurements were carried out manually on the surface of 10 mL solutions located in a thermostatically controlled cell. Surface tension was measured until a constant value was obtained indicating equilibrium. The concentration dependences of the surface tension represent the average value of all measurements, and the error was within 2%. Values of cmc were determined at inflection points on the dependence of surface tension on the logarithm of surfactant concentration. From the tensiometric data, thermodynamic parameters of surfactant interfacial adsorption and micelle formation can be obtained [42,43]. The surface excess, Γ_{max}, and the surface area per a molecule, A_{min}, have been calculated using the Gibbs equation:

$$\Gamma_{max} = \frac{1}{2.3nRT} \lim (d\pi / d\log C_{C \to cmc})$$

$$A_{min} = 10^{18}/(N_A \times \Gamma_{max})$$

where $R = 8.31$ J mol^{-1} K^{-1} (gas constant), π is the surface pressure obtained from the surface tension of water minus the surface tension of the surfactant solution, and T is the absolute temperature in K. N_A is Avogadro number (6.02×10^{23} mol^{-1}). The parameter n represents the number of species at the interface the concentration of which changes with surfactant concentration. The constant n takes the value 2 for monomeric surfactants. C is the surfactant concentration.

The value of the standard free energy of micellization (ΔG_m) was calculated according to equation:

$$\Delta G_m = (1 + \beta) RT \ln (cmc)$$

where β is degree of counterions binding, cmc is the concentration corresponding to the onset of aggregation, i.e. the molar concentration of surfactants in monomeric (non-micellized) form.

The standard free energy of adsorption (ΔG_{ad}) is correlated with the standard free energy of micellization by the following equation:

$$\Delta G_{ad} = \Delta G_m - \frac{\pi_{CMC}}{\Gamma_{max}}$$

2.5. Electrical conductivity measurement

The electrical conductivity (χ, $\mu S \cdot cm^{-1}$) was measured on an InoLab Cond 7110 conductivity meter (WTW, Germany) using a TetraCon sensor. The cmc value was determined by the kink in the graph of the conductivity versus surfactant concentration. The conductivity of water, which was used to prepare the systems under study, was taken as the zero surfactant concentration point.

2.6. Spectrophotometry

Absorption spectra were recorded on a Specord 250 Plus spectrophotometer (Analytik Jena, Germany) using 0.5 and 1 cm thick glass cuvettes. To study the solubilizing ability toward the Orange OT spectral probe, a sample of a dye weighing 0.0014 g was added to all the studied solutions. Then the absorbance was measured at 495 nm. According to the slope of the linear part of the concentration dependences of the reduced optical density at the point of maximum absorption, the solubilization capacity were calculated according to equation:

$S = b/\varepsilon$,

where b is $D/l = f(C)$ dependency slope, ε – an extinction coefficient of Orange OT (17,400 M^{-1} cm^{-1}).

2.7. Dynamic light scattering

The diameter of the aggregates was determined by dynamic light scattering on Zetasizer Nano Instrument (Malvern, UK). The source of laser radiation was a He-Ne gas laser with a power of 4 mW and a wavelength of 633 nm. The effective hydrodynamic diameter was automatically calculated on the device from the diffusion coefficients according to the Stokes-Einstein equation for spherical particles. The obtained experimental data were analyzed using the Malvern DTS program. For each system, the hydrodynamic diameter was determined as the average of at least 5 measurements.

2.8. The Krafft temperature (T_K) measurement

Krafft temperatures were determined using conductometry. Surfactant solutions of certain concentration higher than cmc value but within the surfactant solubility (30 mM for $C_{12}SU$, 20 mM for $C_{14}SU$, 17.5 mM for $C_{16}SU$, 10 mM for $C_{18}SU$) were placed in a freezer at a negative temperature for at least 24 h to reach equilibrium state. Then the temperature was gradually increased using a thermostatic water bath with conductivity measurements each minute. Once the turbid solution became clear, a discontinuity in the conductivity versus temperature plot was taken as the Krafft temperature. The measurements were conducted three times.

2.9. Fluorescence spectroscopy

The fluorescence spectra of pyrene ($1 \cdot 10^{-6}$ mol L^{-1}) in amphiphile solutions were recorded in Hitachi F-7100 spectrofluorimeter (Hitachi, Japan). Sample excitation was at a wavelength of 335 nm. Emission spectra were recorded within 350–500 nm range. The thickness of the cell was 10 × 10 mm. Fluorescence intensities of the first peak at 373 nm (I_I) and of the third peak at 384 nm (I_{III}) of pyrene were obtained from the spectra [44]. The data were analyzed using the Microsoft Excel and Origin Pro 8.5 software.

The aggregation numbers were measured using cetylpyridinium bromide (1 mM stock solution) as a quencher [45]. The peak at 395 nm was used to calculate the aggregation numbers according to the equation:

$$\ln \frac{I_0}{I} = \frac{N_{agg}}{C_{C_nSU} - C_{cmc}} \times C_q$$

where I_0 and I are the fluorescent intensities of pyrene in the absence and the presence of cetylpyridinium bromide; C_q, C_{cmc}, and C_{CnSU} are the concentrations of the quencher, micelles, and C_nSU. Equation was derived under the assumption that the probe and the quencher are entirely present in the micelle phase, their distributions obey the Poisson statistics, and the probe fluoresces only in the absence of the quencher.

2.10. NMR diffusometry

NMR diffusometry experiments were performed on a Bruker AVANCE-500 spectrometer. The spectrometer is equipped with a z-gradient inverse probehead capable of producing gradients with the strength of 50 G cm^{-1}. Experiments were carried out at 40 ± 0.2 °C. Chemical shifts (δ) were reported relative to the solvent as internal standard (HDO $\delta(^1H)$ 4.70 ppm).

The Fourier transform pulsed-gradient spin-echo (FT-PGSE) experiments were performed by BPP-STE-LED (bipolar pulse pair–stimulated echo-longitudinal eddy current delay) sequence [46]. After Fourier transformation and baseline correction, the diffusion dimension was processed with the Bruker TopSpin software package (version 3.2). All separated peaks were analyzed and the average values were presented [47,48]. DOSY ^1H NMR spectra of $C_{10}SU$ (Fig. S7) and $C_{14}SU$ (Fig. S8) are given in SI.

Hydrodynamic radius (R_H) has been calculated from the self-diffusion coefficients D_s applying Stokes-Einstein equation: $R_H = k_BT/6\pi\eta D_s$, where R_H is hydrodynamic radius, k_B is Boltzmann constant, T is the temperature (K), η (Pa·s) is dynamic viscosity of the solvent and D_s is self-diffusion coefficient. The aggregation numbers of C_nSU were estimated from the ratio $N_{agg} = (R_{Ha}/R_{Hm})^3$, where R_{Ha} и R_{Hm} are hydrodynamic radii of the aggregate and monomer C_nSU molecules, respectively.

2.11. Antimicrobial activity

The antibacterial and antifungal activity of the C_nSU were investigated against several pathogenic representative Gram-positive bacteria *Staphylococcus aureus ATCC 209p (Sa), Bacillus cereus ATCC 8035 (Bc)*; Gram-negative bacteria *Escherichia coli CDC F-50 (Ec), Pseudomonas aeruginosa ATCC 9027 (Pa)*; and fungi *Aspergillus niger BKMF-1119 (An), Trichophyton mentagrophytes* var. *gypseum 1773 (Tm), Candida albicans 855–653 (Ca)*. The bacteriostatic and fungistatic activity was studied in Muller Hinton Broth 2 (bacteria 3×10^5 cfu mL^{-1}) and Sabouraud dextrose broth (fungi 2×10^3 cfu mL^{-1}). Chloramphenicol and ketoconazole were used as standard drugs. The results were recorded every 24 h for 5–14 days. Cultures were incubated at 25–37 °C. The experiment was repeated three times. The dilutions of the compounds were prepared immediately in nutrient media; 5% DMSO was added for better solubility and the test strains were not inhibited at this concentration. The minimum inhibitory concentration (MIC) was defined as the minimum concentration of a compound that inhibits the growth of the corresponding test microorganism. The minimum bactericidal (MBC) and fungicidal (MFC) concentrations were determined by adding an aliquot of the bacterial (fungal) culture to Mueller-Hinton or Sabouraud dextrose agar in a 10 cm Petri dish and incubated for 24–48 h at 25–37 °C. MBC and MFC were the minimum concentration in which bacterial colonies were not detected, indicating that bacteria were killed with an efficiency of >99.9% [49].

2.12. Hemolytic activity

Series of C_nSU surfactants were evaluated in terms of hemolytic activity by comparing the optical density of C_nSU treated erythrocyte suspension with the optical density of blood at 100% hemolysis [50]. 10% suspension of human erythrocytes was used as an object of investigation. An erythrocytic mass was treated with heparin and washed thrice with physiological saline (p.sal., 0.9% NaCl), centrifuged for 10 min at

800 rpm, and resuspended in p.sal. to make a 10% suspension. The concentrations of the surfactants that correspond to the MIC values for the bacterial test strains were prepared in saline (supplemented with 5% DMSO), and 450 μL of the compound at the corresponding dilution was added to 50 μL erythrocyte suspension. The samples were treated for 1 h at 37 °C and then centrifuged for 10 min at 2000 rpm. Released hemoglobin was controlled by measuring the optical density of the supernatant on Microplate reader Invitrologic (Russia) at 540 nm. Control sample with 0% hemolysis was prepared by adding of 50 μL of 10% erythrocyte suspension to 450 μL of p.sal., and the 100% hemolysis control sample was prepared by adding of 50 μL of 10% red blood cell suspension to 450 μL of distilled water.

3. Results and discussion

3.1. Krafft temperature (T_K) of C_nSU series

Isothiuronium cationic surfactants starting with $C_{14}SU$ have limited solubility in water. So, their Krafft temperatures were determined (Fig. 3) using the conductometry method in order to select the operating temperature range for self-assembly studies. Linear fitting was applied to lower and upper parts of the curves and the Krafft temperature was taken as the intersection point x-axis value (Fig. 3). The linear fit equations from which the temperature was determined as the intersection are the following:

$C_{14}SU$: $y = 73 + 2.7x$ (lower part); $y = -615 + 22x$ (upper part)

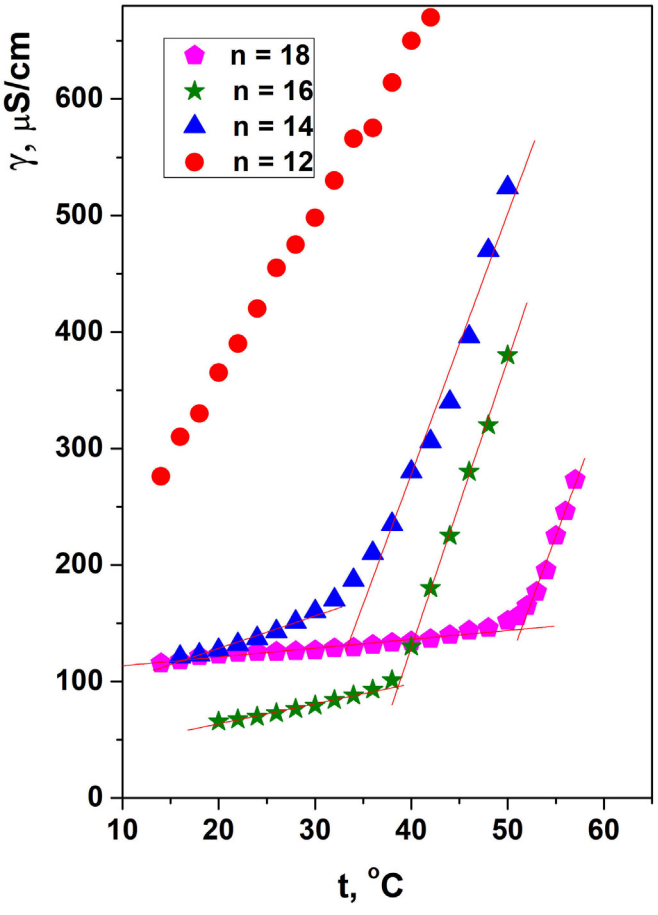

Fig. 3. The dependence of the electrical conductivity of C_nSU aqueous solutions on the temperature, that was used to estimate the Krafft temperature of surfactants.

$C_{16}SU$: $y = 29 + 1.72x$ (lower part); $y = -885 + 24,6x$ (upper)

$C_{18}SU$: $y = 106 + 0.758x$ (lower part); $y = -1000 + 22x$ (upper)

The approach is based on the fact that the electrical conductivity of a slowly defrosting solution increases with increasing temperature due to the dissolution of surfactants [51,52]. For $C_{12}SU$, the exact value of the Krafft temperature could not be determined, since it turned out to be less than 10°C. Since the Krafft temperature increases with increasing length of the surfactant alkyl tail, we hypothesized that $C_{10}SU$ also has a low T_K. For $C_{14}SU$ and $C_{16}SU$, the Krafft temperature is 36°C and 39°C (Table 1), respectively. It is worth noting that these are quite high T_K values. For example, for the classic series of alkyltrimethylammonium bromides with tetradecyl and hexadecyl substituents, the Krafft temperature is 0°C and 25°C, respectively [52]. The Krafft temperature for $C_{18}SU$ is 51°C (Table 1), which significantly limits its application from a practical point of view, therefore, further studies with this representative of the series were not carried out. It is known that the Krafft temperature is affected by two main factors: the solubility of surfactant monomers and intermolecular attraction in the hydrocarbon regions of crystals or in layers of polar groups. The obtained low T_K values for the decyl and dodecyl derivatives indicate the availability of nitrogen lone pair of the surfactant head group for the formation of hydrogen bonds, which leads to good solubility of the surfactant. When passing to higher homologs, an increase in intermolecular interaction of hydrophobic fragments in the crystalline state probably occurs, which is reflected in high T_K values.

Next, self-assembly study of a new homologous series of amphiphilic isothiuronium salts was carried out using a wide range of physicochemical methods: tensiometry, conductometry, fluorimetry, spectrophotometry, dynamic light scattering and NMR diffusometry, each of which provide their own insight into the aggregation behavior of surfactant molecules. Tensiometric data are used to obtain thermodynamic parameters of micelle formation and interfacial adsorption. Solubilization data are helpful to assess the ability of the aggregates formed by the surfactants in study to act as drug nanocarriers. With some considerations, aggregation numbers can also be obtained from solubilization data. Fluorimetry data provide details on the polarity inside the micellar core and aggregation numbers.

3.2. Tensiometry and conductometry data

It was found that the Krafft temperature for $C_{16}SU$ is 39°C, therefore, in order to conduct a comparative analysis within the homologous series of surfactants, all the dependences were obtained at 40°C.

Tensiometry and conductometry are traditionally used to determine the cmc. The tensiometry method is based on the ability of a surfactant to reduce surface tension. With an increase in surfactant concentration, surface tension decreases sharply, and after reaching a cmc, it remains constant. The dependence of the surface tension C_nSU as a function of the concentration of the amphiphilic compound in an aqueous solution

Table 1
Krafft temperature and critical micelle concentrations of C_nSU determined by tensiometry and conductometry.

Surfactants	cmc × 10^3 (M)		Krafft point (°C)
	Tensiometry	Conductometry	
$C_{10}SU$	16	18	–
$C_{12}SU$	4	5	< 10
$C_{14}SU$	1.3	1.8	36
$C_{16}SU$	0.5	0.45	39

at 40°C is shown in Fig. 4,A: for all surfactants, the surface tension gradually decreases to a plateau with a value of about 30 mN m^{-1}. The cmc values obtained from the tensiometric dependences are presented in Table 1. As expected, an increase in the length of the alkyl tail from 10 to 16 carbon atoms leads to a decrease in the cmc values from 16 to 0.5 mM. The logarithm of the obtained cmc values on the number of carbon atoms in the alkyl tail is characterized by a linear dependence (Fig. 5): $y = 0.6567–0.25x$ ($r^2 = 0.9895$).

Using the surface tension isotherms of micellar systems, the thermodynamic characteristics of the surface layer were calculated, the values of which are summarized in Table 2. The obtained values of surface area per surfactant molecule (A_{min}) are in agreement with their structure and remain at the same level for surfactants with different hydrocarbon chain lengths. For comparison, the CTAB has an area of about 0.32 nm^2. The obtained areas of the order of 1 nm^2 may be reasonable, if we consider that the CTAB head group is sterically hindered at all the sides except the top, so hydration is occurring axially, which does not allow for additional water molecules that would increase the head group equilibrium cross-section area. In the case of C_nSU, the area is noticeably larger, firstly, due to the larger structure of the head group, and secondly, because it does not have hydrophobic methyl groups, which allows for attachment of water molecules that contribute to the head group cross section area. The delocalized nature of the C_nSU head groups allows for more hydrogen bonds from all the sides, which in turn make the equilibrium head group area larger. These assumptions are not supported by physicochemical methods in the current work,

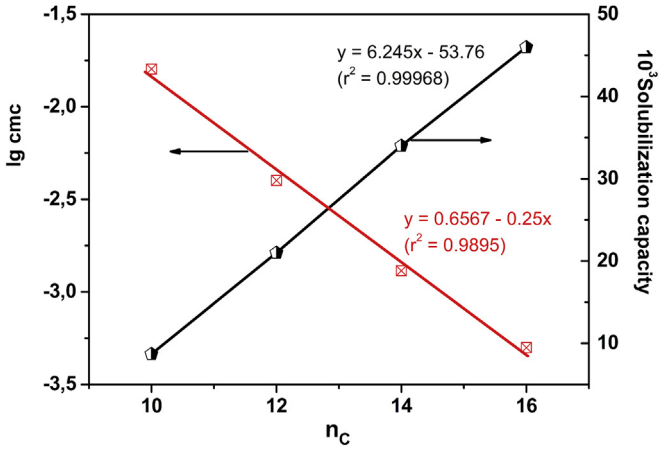

Fig. 5. The logarithm of cmc and solubilization capacity of C_nSU surfactants toward Orange OT versus the number of carbon atoms, 40°C.

however an x-ray study has previously shown that thiourea group by itself can readily form hydrogen bonds [53]. The values of adsorption energy tend to obtain more negative values with an increase in the number of hydrophobic carbon atoms in C_nSU molecules. This is due to the fact that longer hydrophobic parts of surfactants represent a

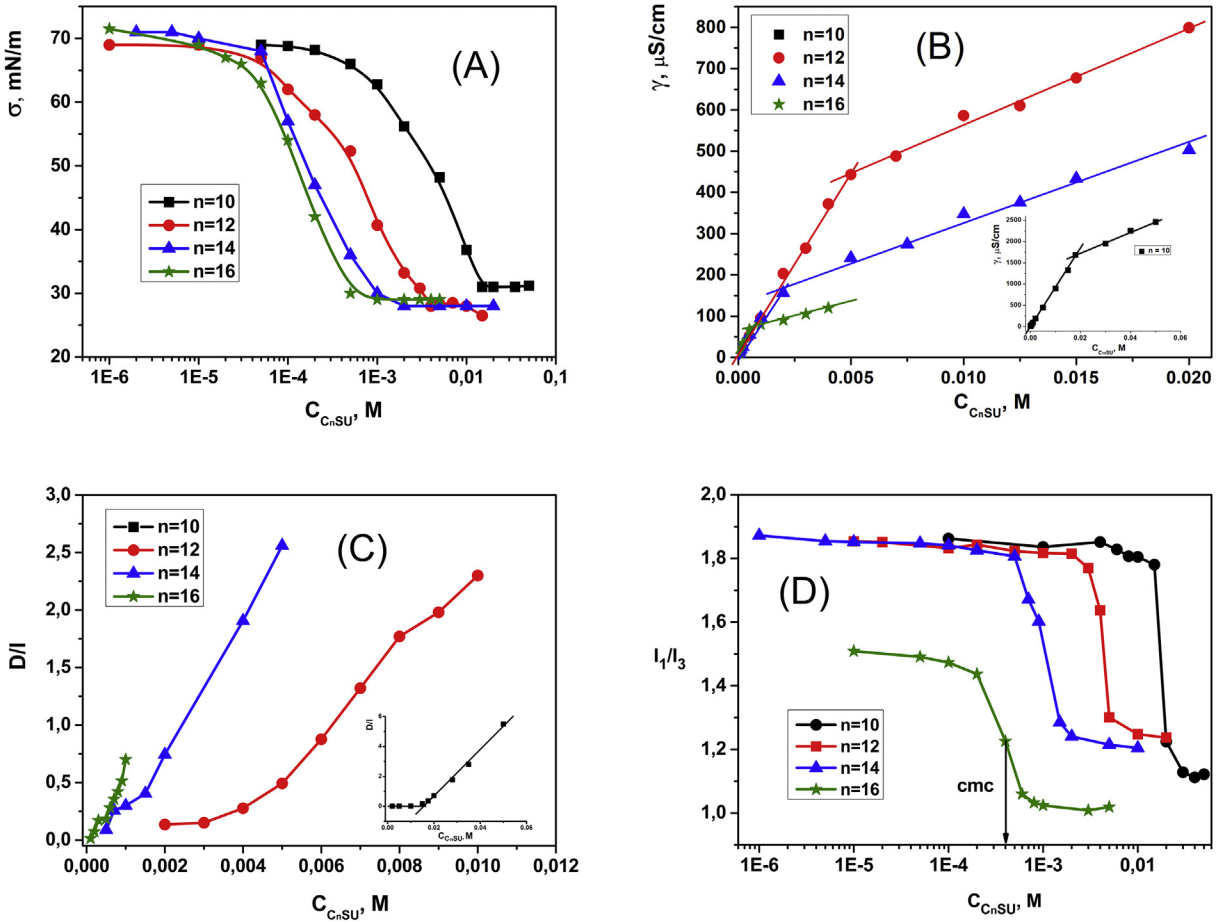

Fig. 4. The obtained plots that were used for determination of cmc values with various methods: (A) tensiometry, (B) conductometry (the inset shows the dependence for $C_{10}SU$), (C) Orange OT solubilization (the inset shows the dependence for $C_{10}SU$), λ = 495 nm, (D) spectrofluorimetry, C(pyrene) = 1×10^{-6} M. All of these measurements were made in H_2O at 40°C.

Table 2
Values of surface excess (Γ_{max}), surface area per surfactant molecule (A_{min}), standard free energy of micellization (ΔG_m) and the standard free energy of interfacial adsorption at the air/saturated monolayer interface (ΔG_{ad}) of isothiuronium surfactants, from tensiometry data obtained at 40 °C.

Surfactants	Γ_{max} x 10^6 ($mol \cdot m^{-2}$)	A_{min} (nm^2)	$-\Delta G_{ad}$ ($kJ \cdot mol^{-2}$)	$-\Delta G_m$ ($kJ \cdot mol^{-2}$)
$C_{10}SU$	1.47	1.1	38.9	16.4
$C_{12}SU$	2.44	0.9	44.7	26.7
$C_{14}SU$	1.87	0.9	44.5	26.4
$C_{16}SU$	1.60	1.0	47.7	30.2

larger water displacement due to their volume. Therefore, the processes of micelle formation and adsorption for longer surfactants are more favorable than for short ones.

Conductometry also shows aggregation in the systems under study. It is known that the mobility of individual unassociated ions is significantly higher than the mobility of aggregated ions. This phenomenon is the basis of the conductometric method [54]. Fig. 4,B shows the dependences of the electrical conductivity (χ) of a series of surfactants under study at 40°C. For each surfactant, the results fit into two straight lines with different slopes. In the region of low concentration, the change in electrical conductivity can be attributed to a higher concentration of free cations and anions of C_nSU, while the inflection point can be attributed to the onset of micelle formation (cmc values are presented in Table 1). After cmc, the change in electrical conductivity has a lower slope, which can be explained in two ways: (1) by immobilizing the fraction of counterions around the surface of the micelles, which effectively reduces the number of free bromide anions; (2) micelles are less likely to promote charge transfer than free cations of surfactant monomers due to their lower mobility. The obtained values are in good agreement with the tensiometric data.

3.3. Solubilization properties of C_nSU

The solubilization of hydrophobic compounds in micelles is the most important property of surfactants, which determines their practical application. In addition, solubilization of model spectral probes makes it possible to determine the cmc values. The method is based on two observations: (1) at a solution concentration below cmc, the dye is practically not soluble; (2) when the cmc is reached, the solubility of the dye increases sharply [55]. The ability of C_nSU aggregates to act as nanocontainers was demonstrated with hydrophobic dye Orange OT as a probe, which has a characteristic band in the visible region at 495 nm. The absorption spectra of Orange OT in C_nSU micellar solution at 40°C are shown in Fig. S9. The dependences of the reduced optical density on the surfactant concentration (Fig. 4,C) show points of a sharp increase in optical density, which can be attributed to cmc points (Table 3). The cmc determined by the solubilization method for $C_{10}SU$ and $C_{12}SU$ at 25°C (Figs. S10, S11) practically do not differ from the cmc at 40°C (Table 3).

The solubilization capacity values (the number of moles of dye solubilized per mole of surfactant) are given in Table 3, which are 2–3 times higher than for alkylammonium analogues [51]. An increase in temperature from 25 to 40°C leads to an increase in solubilization capacity from 0.0072 to 0.0087. These data can also be used to calculate aggregation numbers by taking into account the extinction coefficient of the dye and making an assumption that only one hydrophobic molecule is being solubilized per aggregate [56]. The dependence of the solubilization capacity on the number of carbon atoms in the alkyl tail is characterized by a linear dependence (Fig. 5) with a good correlation coefficient: $y = 6.245\times - 53.76$ ($r^2 = 0.99968$).

3.4. Fluorescence data. DLS data

The study of the behavior of a series of isothiuronium surfactants in aqueous solutions was supplemented by the results of the method of fluorimetry using pyrene. This method is widely used to study the properties of surfactants, due to its high sensitivity and a very low concentration of the introduced fluorophore, and it allows to determine the micropolarity of the medium around the probe, the cmc value and the aggregation numbers [57,58]. For $C_{10}SU$ and $C_{12}SU$, which have good solubility at 25°C, these parameters were determined at two temperatures: 25°C and 40°C. For the other homologs, measurements were done at 40°C.

Pyrene has a spectrum with 5 characteristic peaks. The first (I_I) and third (I_{III}) peaks are very sensitive to the polarity of the microenvironment, therefore, when the solvent is replaced, their intensities change. In a polar medium (in water) the I_I/I_{III} ratio (polarity parameter) is in the range of 1.8–2.0, and in a non-polar medium (for example, hexane), around 0.6. With the addition of amphiphile with an increase in its concentration, the overall polarity of the pyrene environment decreases, due to its localization in the micellar hydrophobic core. Fig. 4,D shows the dependences of the polarity parameter on the concentration of C_nSU at 40°C, which were plotted from the fluorescence spectra of pyrene in the presence of increasing concentrations of isothiuronium surfactants (Fig. S12). From the dependencies shown in Fig. 4D, the cmc values were determined, which are consistent with the cmc values obtained by other methods. For $C_{10}SU$ and $C_{12}SU$, the cmc values determined at 25°C (Figs. S13, S14) practically do not differ from those obtained at 40°C. This can be explained by the complex dependence of the cmc on temperature, which can be simultaneously influenced by several factors that cancel each other out. The cmc values obtained by fluorimetry are presented in Table 3.

At a fixed surfactant concentration (twice the cmc value), aggregation numbers (N_{agg}) were determined using cetylpyridinium bromide as a quencher. The quenching spectra of pyrene fluorescence in the presence of cetylpyridinium bromide are shown in Figs. S15, S16. According to the obtained spectra, linearization was carried out and the aggregation numbers were calculated from the slope angles (Fig. 6). Since two representatives of the series ($C_{10}SU$ and $C_{12}SU$) are soluble both at 25°C and 40°C, the aggregation numbers were calculated at two temperatures.

Table 3
The cmc values and aggregation numbers derived from the fluorescence and the dye solubilization study. *Z*-Average from DLS.

Surfactants	T (°C)	cmc × 10^3 (M)		S × 10^3	Aggregation number by dye solubilization	Aggregation number by fluorescence, (2 x cmc, M)	Z-Average (d, nm)
		Pyrene fluorescence	Orange OT solubilization				
$C_{10}SU$	25	16.5	15	7.2	–	76 (0.033)	–
	40	16	16	8.7	110	106 (0.032)	366
$C_{12}SU$	25	3.2	4.1	19	–	80 (0.0063)	–
	40	3.1	4.4	21	37	90 (0.0062)	285
$C_{14}SU$	40	1.1	1.5	34	23	36 (0.0022)	157
$C_{16}SU$	40	0.4	0.45	46	15	6 (0.0008)	135

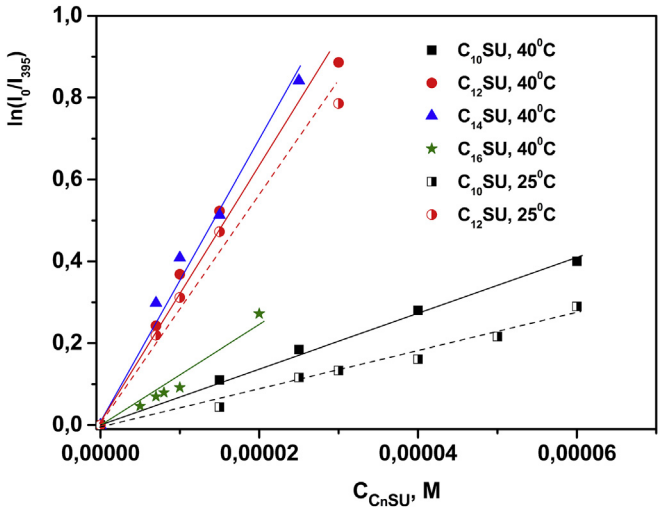

Fig. 6. The ratio of fluorescence intensity of pyrene vibronic peak at 395 nm in the absence and the presence of cetylpyridinium bromide vs quencher concentration, that was used to obtain aggregation numbers; C(pyrene) = 1×10^{-6} M, H_2O. Temperatures are given on the graph legend. The fluorescence spectra are shown in Figs. S15, S16.

It was established that an increase in the length of the alkyl tail in the series C_{10}SU - C_{12}SU - C_{14}SU - C_{16}SU leads to a decrease in the aggregation numbers from 106 to 6 (Table 3). This trend is confirmed by data obtained from the dye solubilization study given in Table 3 for comparison. The N_{agg} can be roughly estimated from the absorbance of C_nSU solutions saturated with Orange OT (Fig. 4,C) by making the following assumptions: (a) the solubilization ratio is one micelle per dye molecule; (b) the concentration of detergent not associated into micelles is constant and equal to the cmc [59]. The decrease in the N_{agg} with increase in the length of the alkyl tail is nontypical for classical surfactants, for example, for a series of alkyltrimethylammonium bromides, it has been shown that the aggregation numbers are 55 (C_{12}TAB), 70 (C_{14}TAB), and 89 (C_{16}TAB) [44]. Aggregation number of alkyl pyrrolidinium bromides (L-C_nPB) obtained from steady-state fluorescence quenching was found to be 42, 48, and 53 for L-C_{12}PB, L-C_{14}PB, and L-C_{16}PB, respectively [60]. However, upon the transition to cationic surfactants with a more voluminous structure of the head group, the opposite tendency in the change of aggregation numbers can be observed. For example, this was shown for a series of triphenylphosphonium surfactants [61] and quaternary ammonium derivatives of quinuclidine [62]. However, it is assumed that the CN_2S core is planar, therefore, it is not possible to explain the decrease in aggregation numbers from the point of view of the volume head group.

Therefore, the dynamic light scattering method was additionally used to determine the hydrodynamic diameter of the aggregates in aqueous C_nSU solutions at a concentration twice as large as cmc. It was found that for the C_nSU series the hydrodynamic diameter averaged over the number of particles is 50–70 nm (Figs. S17-S20). These values are not typical for classical micellar aggregates, which suggests the formation of aggregate through another packing model. It is also worth noting that the hydrodynamic diameter averaged over intensity (Figs. S17-S20) has a bimodal distribution: 50–70 nm and about 300 nm. That is, the calculated aggregation numbers are effective and reflect contributions by at least two types of particles. Importantly, the values of *Z*-Average (Table 3) decrease with increasing length of the surfactant alkyl tail, which indicates the predominance of smaller aggregates and is in good agreement with a decrease in aggregation numbers.

3.5. NMR diffusometry data

To further specify aggregation behavior two representatives of the homologous series, namely, C_{10}SU and C_{14}SU, were studied by NMR diffusion measurements (Fig. 7, Tables S1, S2). As previously shown, NMR-self-diffusion technique is very sensitive to the formation of small spherical micelles, including pre-micellar aggregates [51], which is valuable information in case of different morphology of aggregates assumed. As can be seen in Fig. 7, a sharp inflection point can be observed in the self-diffusion coefficient plot, which indicates the formation of aggregates with low mobility compared to free surfactant molecules. Aggregate sizes and aggregation number values were calculated as function of surfactant concentration (Tables S1, S2). It should be noted that for C_{14}SU, the formation of pre-micellar aggregates, dimers, is shown at a concentration of 0.75 mM (before the cmc value). Aggregate sizes for both surfactants studied increase with an increase in surfactant concentration, with hydrodynamic diameter reaching ca.2 to 6 nm. Probably this is due to the contribution of small micelle-like particles that represent the beginning of self-assembly of the systems.

For C_{14}SU, aggregation numbers increase up to 40 (Table S1) at a concentration of 5 mM (3.8 times greater than the tensiometric cmc). This is consistent with values found by fluorimetry, provided that no structural changes occur in this concentration range, and this is not in essential contradiction with the dye solubilization results. For C_{10}SU, the aggregation numbers determined by NMR are significantly lower than those determined by fluorimetry and dye solubilization techniques. This can be due to several reasons, namely, (i) fluorescence and dye solubilization techniques detect data based on aggregates that contain probes in their composition, which can significantly alter the morphological behavior, especially in the lower concentrations range (ii) high sensitivity of NMR-self-diffusion method to the occurrence of small micelle-like aggregates and pre-micellar assemblies; (iii) incompact packing mode of aggregates, which may result in averaging of self-diffusion coefficients due to exchange of surfactant molecules between aggregated and monomer state under the conditions of relatively long NMR-self-diffusion experiments of 50 ms.

3.6. Antimicrobial and hemolytic action

The antimicrobial activity of C_nSU surfactants was tested against gram-positive bacteria *Staphylococcus aureus ATCC 209p (Sa)* and *Bacillus cereus ATCC 8035 (Bc);* gram-negative bacteria *Escherichia coli CDC F-50 (Ec)* and *Pseudomonas aeruginosa ATCC 9027 (Pa);* fungi *Aspergillus niger BKMF-1119 (An), Trichophyton mentagrophytes* var. *gypseum 1773 (Tm),* and *Candida albicans 855–653 (Ca).* The minimum inhibitory concentrations, the minimal bactericidal concentrations and the minimal fungicidal concentrations are summarized in Table 4. Bacteriostatic

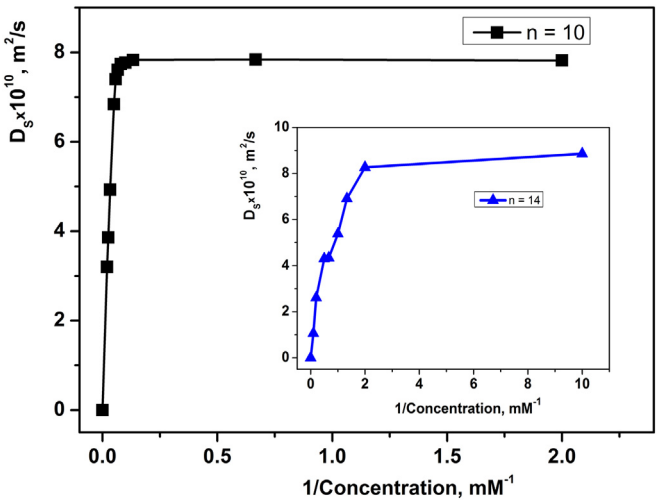

Fig. 7. The self-diffusion coefficient of cationic surfactants C_{10}SU and C_{14}SU vs. reciprocal surfactant concentration at 40 °C in D_2O.

Table 4
Antimicrobial activity of C_nSU.*

Surfactants	Bacteriostatic and fungistatic activity MIC (μg·mL^{-1})						
	Sa	*Bc*	*Ec*	*Pa*	*An*	*Tm*	*Ca*
$C_{10}SU$	15.6 ± 1.2	15.6 ± 1.4	>500	>500	>500	>500	62.5 ± 5.6
$C_{12}SU$	15.6 ± 1.2	15.6 ± 1.3	>500	>500	>500	>500	62.5 ± 5.3
$C_{14}SU$	15.6 ± 1.3	15.6 ± 1.2	>500	>500	>500	>500	15.6 ± 1.4
$C_{16}SU$	31.3 ± 2.6	62.5 ± 5.7	>500	>500	>500	>500	31.3 ± 2.7
CTAB**	0.5	3.1	6.3	250	62.5	31.3	3.1
Chloramphenicol	62.5 ± 5.6	62.5 ± 5.7	125 ± 10	–	–	–	–
Ketoconazole	–	–	–	–	–	4.0 ± 0.3	4.0 ± 0.3
	Bactericidal and fungicidal activity MBC, MFC (μg·mL^{-1})						
$C_{10}SU$	62.5 ± 5.8	31.3 ± 2.5	>500	>500	>500	>500	125 ± 11
$C_{12}SU$	62.5 ± 5.4	62.5 ± 5.3	>500	>500	>500	>500	62.5 ± 5.6
$C_{14}SU$	62.5 ± 5.8	62.5 ± 5.4	>500	>500	>500	>500	62.5 ± 5.3
$C_{16}SU$	250 ± 21	125 ± 10	>500	>500	>500	>500	125 ± 10
CTAB**	50	>500	>500	>500	>500	>500	50

* Average of three values measured; ± standard deviation (SD).
** From [63].

activity of test compounds is more expressed than bactericidal. It can be seen that all compounds demonstrate antimicrobial activity against test strains of gram-positive bacteria *S. aureus 209p* and *B. cereus 8035* and the yeast-like fungus *C. albicans 855–653*. By bacteriostatic activity $C_{10}SU$ - $C_{14}SU$ compounds are 4 times superior to the comparison drug chloramphenicol (bacteriostatic drug) against *S. aureus 209p* and *B. cereus 8035*. $C_{16}SU$ was less active, but also showed antibacterial activity at the level of the reference drug. In experiments with gram-negative bacteria, the tested compounds in the studied concentrations did not exhibit antimicrobial properties. Surfactants $C_{12}SU$ and $C_{14}SU$ have a fungicidal effect at a concentration of 62.5 μg·mL^{-1} toward the yeast-like fungus *C. albicans*. Against *T. mentagrophytes* and *A. niger* all compounds were inactive. Compared to the classical cationic surfactant cetyltrimethylammonium bromide isothiuronium series has been less active toward all studied bacterial strains, which was assessed previously in the same workspace as the surfactants in study [63].

Hemolysis with surfactant molecules is a process of great fundamental and practical importance. Hemolytic activity of surfactants can be used as a criterion for their toxicological assessment [64]. Thus, in the summary round of our investigation the hemolytic activity of C_nSU compounds was studied. Fig. 8 presents data on the assessment of the degree of hemolysis of human red blood cells caused by the studied compounds in the concentration range of 15.6–250 μg·mL^{-1}. The MIC values of the tested compounds are in this range. It can be seen that all compounds in the studied concentrations have lower hemolytic activity than the antibiotic Gramicidin S, which is known to cause erythrocyte hemolysis and therefore cannot be used for intravenous administration. Yet, due to the sufficiently high antimicrobial activity, it is widely used in medicine for external treatment [65]. The hemolysis caused by $C_{10}SU$ and $C_{12}SU$ at a concentration of 15.6 μg·mL^{-1} does not exceed 1%, that is, they may be of interest for further research with living objects.

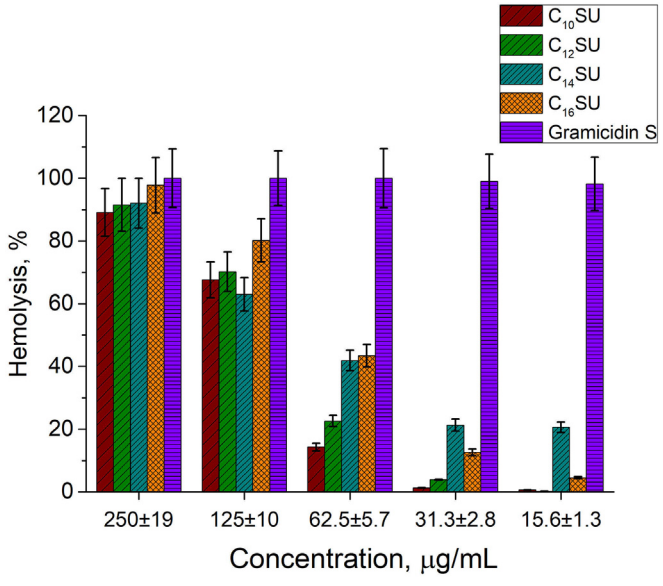

Fig. 8. Hemolytic activity of C_nSU surfactants.

4. Conclusion

A series of surfactants bearing an isothiuronium head group (C_nSU, where $n = 10, 12, 14, 16, 18$) were synthesized and characterized by IR, NMR, elemental analysis. For the first time it is shown that such surfactants contain a double bond in the head group, which was evident from x-ray data. Krafft temperature and critical micelle concentration are obtained by methods of tensiometry, conductometry, spectrophotometry, fluorimetry. Physicochemical characterization has shown that the C_nSU surfactants have 2–3 times higher solubilization capacity than alkyltrimethylammonium analogues. They tend to form aggregates of different sizes, with DLS study testifying the larger size population, while NMR diffusometry the contribution of smaller micelle-like population. The aggregation numbers for C_nSU were calculated by fluorimetry, dye solubilization and NMR self-diffusion methods. The transition from $C_{10}SU$ to $C_{16}SU$ is accompanied by a decrease in aggregation numbers. C_nSU surfactants demonstrate antimicrobial activity against test strains of gram-positive bacteria *S. aureus 209p* and *B. cereus 8035* and the yeast-like fungus *C. albicans 855–653*, with no hemolytic activity observed.

Declaration of Competing Interest

The authors declare that they have no known competing financial interests or personal relationships that could have appeared to influence the work reported in this paper.

Acknowledgment

This work in the part of the study of self-organization, solubilization and biological activity of isothiuronium surfactants was supported by Russian Science Foundation (project № 19-73-30012) for V.F.G., P.R.V.,

G.G.A., V.A.D., Z.L.Ya. This work in the part of synthesis of isothiuronium surfactants was funded by the subsidy allocated to Kazan Federal University for the state assignment in the sphere of scientific activities № 0671-2020-0063 for G.I.V. and B.D.I. X-ray single crystal study and NMR experiment were supported from the government assignment for FRC Kazan Scientific Centre of RAS for I.K.A. and K.O.N. The authors gratefully acknowledge the CSF-SAC FRC KSC RAS for providing necessary facilities to carry out this work.

Appendix A. Supplementary data

Supplementary data to this article can be found online at https://doi.org/10.1016/j.molliq.2020.114721.

References

[1] M. Damen, A.J.J. Groenen, S.F.M. Van Dongen, R.J.M. Nolte, B.J. Scholte, M.C. Feiters, Transfection by cationic gemini lipids and surfactants, Medchemcomm 9 (2018) 1404–1425, https://doi.org/10.1039/C8MD00249E.

[2] L.Y. Zakharova, T.N. Pashirova, S. Doktorovova, A.R. Fernandes, E. Sanchez-Lopez, A.M. Silva, S.B. Souto, E.B. Souto, Cationic surfactants: self-assembly, structure-activity correlation and their biological applications, Int. J. Mol. Sci. 20 (2019) 1–31, https://doi.org/10.3390/ijms20225534.

[3] N. Zhang, A.V. Nguyen, C. Zhou, A review of the surface features and properties, surfactant adsorption and floatability of four key minerals of diasporic bauxite resources, Adv. Colloid Interf. Sci. 254 (2018) 56–75, https://doi.org/10.1016/j.cis.2018.03.005.

[4] M. Lokanathan, H. Sharma, M. Shabaka, V. Bahadur, K. Mohanty, Comparing electrowettability and surfactants as tools for wettability enhancement on a hydrophobic surface, ASME Int. Mech. Eng. Congr. Expo. Proc. 7 (2019) 124155, https://doi.org/10.1016/j.colsurfa.2019.124155.

[5] S. Liu, X. Liu, Z. Guo, Y. Liu, J. Guo, S. Zhang, Wettability modification and restraint of moisture re-adsorption of lignite using cationic gemini surfactant, Colloids Surfaces A Physicochem. Eng. Asp. 508 (2016) 286–293, https://doi.org/10.1016/j.colsurfa.2016.08.073.

[6] S.K. Yadav, K. Parikh, S. Kumar, Mixed micelle formation of cationic gemini surfactant with anionic bile salt: a PAH solubilization study, Colloids Surfaces A Physicochem. Eng. Asp. 522 (2017) 105–112, https://doi.org/10.1016/j.colsurfa.2017.02.048.

[7] R. Saha, A. Ghosh, B. Saha, Kinetics of micellar catalysis on oxidation of p-anisaldehyde to p-anisic acid in aqueous medium at room temperature, Chem. Eng. Sci. 99 (2013) 23–27, https://doi.org/10.1016/j.ces.2013.05.043.

[8] Y.R. Katre, S. Patil, A.K. Singh, Effect of cationic micelle on the kinetics of oxidation of citric acid by N-bromophthalimide in acidic medium, J. Dispers. Sci. Technol. 30 (2009) 159–165, https://doi.org/10.1080/01932690802498070.

[9] C. Zhou, Y. Wang, Structure–activity relationship of cationic surfactants as antimicrobial agents, Curr. Opin. Colloid Interface Sci. 45 (2020) 28–43, https://doi.org/10.1016/j.cocis.2019.11.009.

[10] T.N. Pashirova, E.A. Burilova, S.S. Lukashenko, N.K. Gaysin, O.I. Gnezdilov, A.S. Sapunova, A.R. Fernandes, A.D. Voloshina, E.B. Souto, E.P. Zhiltsova, L.Y. Zakharova, Nontoxic antimicrobial micellar systems based on mono- and dicationic Dabco-surfactants and furazolidone: structure-solubilization properties relationships, J. Mol. Liq. 296 (2019) 112062, https://doi.org/10.1016/j.molliq.2019.112062.

[11] M.E. Fait, L. Bakas, G.L. Garrote, S.R. Morcelle, M.C.N. Saparrat, Cationic surfactants as antifungal agents, Appl. Microbiol. Biotechnol. 103 (2019) 97–112, https://doi.org/10.1007/s00253-018-9467-6.

[12] M.A. Hegazy, A.Y. El-Etre, M. El-Shafaie, K.M. Berry, Novel cationic surfactants for corrosion inhibition of carbon steel pipelines in oil and gas wells applications, J. Mol. Liq. 214 (2016) 347–356, https://doi.org/10.1016/j.molliq.2015.11.047.

[13] L. Chen, H. Xie, Y. Li, W. Yu, Applications of cationic gemini surfactant in preparing multi-walled carbon nanotube contained nanofluids, Colloids Surfaces A Physicochem. Eng. Asp. 330 (2008) 176–179, https://doi.org/10.1016/j.colsurfa.2008.07.047.

[14] M.T. García, I. Ribosa, I. Kowalczyk, M. Pakiet, B. Brycki, Biodegradability and aquatic toxicity of new cleavable betainate cationic oligomeric surfactants, J. Hazard. Mater. 371 (2019) 108–114, https://doi.org/10.1016/j.jhazmat.2019.03.005.

[15] O. Kaczerewska, R. Martins, J. Figueiredo, S. Loureiro, J. Tedim, Environmental behaviour and ecotoxicity of cationic surfactants towards marine organisms, J. Hazard. Mater. 392 (2020) 122299, https://doi.org/10.1016/j.jhazmat.2020.122299.

[16] D.R. Gabdrakhmanov, E.A. Vasilieva, M.A. Voronin, D.A. Kuznetsova, F.G. Valeeva, A.B. Mirgorodskaya, S.S. Lukashenko, V.M. Zakharov, A.R. Mukhitov, D.A. Faizullin, V.V. Salnikov, V.V. Syakaev, S.K. Latypov, Y.F. Zuev, L.Y. Zakharova, Soft Nanocontainers based on Hydroxyethylated Geminis: role of spacer in self-assembling, Solubilization, and Complexation with oligonucleotide, J. Phys. Chem. C 124 (2020) 2178–2192, https://doi.org/10.1021/acs.jpcc.9b10079.

[17] A.R. Tehrani-Bagha, K. Holmberg, Cationic ester-containing gemini surfactants: physical-chemical properties, Langmuir. 26 (2010) 9276–9282, https://doi.org/10.1021/la1001336.

[18] L. Zhi, Q. Li, Y. Li, Y. Sun, Self-aggregation and antimicrobial activity of saccharide-cationic surfactants, Colloids Surfaces A Physicochem. Eng. Asp. 456 (2014) 231–237, https://doi.org/10.1016/j.colsurfa.2014.05.042.

[19] J.I. Garza-Arévalo, A. Intiso, A. Proto, F. Rossi, M. Sanchez-Dominguez, Trichloroethylene solubilization using a series of commercial biodegradable ethoxylated fatty alcohol surfactants, J. Chem. Technol. Biotechnol. 94 (2019) 3523–3529, https://doi.org/10.1002/jctb.5965.

[20] M. Pisárčik, M. Polakovičová, M. Markuliak, M. Lukáč, F. Devínsky, Self-assembly properties of cationic gemini surfactants with biodegradable groups in the spacer, Molecules 24 (2019)https://doi.org/10.3390/molecules24081481.

[21] D. Xu, X. Ni, C. Zhang, J. Mao, C. Song, Synthesis and properties of biodegradable cationic gemini surfactants with diester and flexible spacers, J. Mol. Liq. 240 (2017) 542–548, https://doi.org/10.1016/j.molliq.2017.05.092.

[22] M.C. Morán, A. Pinazo, L. Pérez, P. Clapés, M. Angelet, "Green" amino acid-based surfactants, 2004 233–240.

[23] A.B. Mirgorodskaya, R.A. Kushnazarova, S.S. Lukashenko, L.Y. Zakharova, Self-assembly of mixed systems based on nonionic and carbamate-bearing cationic surfactants as a tool for fabrication of biocompatible nanocontainers, J. Mol. Liq. 292 (2019).

[24] M. Di Bella, A. Tait, C. Parenti, M. Bondi, G. Quaglio, S-aryl(tetramethyl) isothiouronium salts as possible antimicrobial agents, I, Arch. Pharm. (Weinheim). 319 (1986) 451–456, https://doi.org/10.1002/ardp.19863190513.

[25] S. Cohen, I. Laitman, T. Lublin Tennenbaum, M. Natan, E. Banin, S. Margel, Engineering of crosslinked poly(isothiouronium methylstyrene) microparticles of narrow size distribution for antibacterial applications, Polym. Adv. Technol. 28 (2017) 188–192, https://doi.org/10.1002/pat.3873.

[26] A.M. Badawi, E.M.S. Azzam, S.M.I. Morsy, Surface and biocidal activity of some synthesized metallo azobenzene isothiouronium salts, Bioorganic Med. Chem. 14 (2006) 8661–8665, https://doi.org/10.1016/j.bmc.2006.08.021.

[27] W. Dai, W. Yang, Y. Zhang, D. Wang, X. Luo, X. Tu, Novel isothiouronium ionic liquid as efficient catalysts for the synthesis of cyclic carbonates from CO2 and epoxides, J. CO2 Util. 17 (2017) 256–262, https://doi.org/10.1016/j.jcou.2016.12.010.

[28] E. Cho, T.H. Kim, Direct asymmetric aldol reaction co-catalyzed by l-proline and isothiouronium salts, Tetrahedron Lett. 55 (2014) 6470–6473, https://doi.org/10.1016/j.tetlet.2014.10.009.

[29] G.P. Silveira, M. Ferreira, L. Fernandes, G.C. Moraski, S. Cho, C. Hwang, S.G. Franzblau, M.M. Sá, Allylic thiocyanates as a new class of antitubercular agents, Bioorganic Med. Chem. Lett. 22 (2012) 6486–6489, https://doi.org/10.1016/j.bmcl.2012.08.048.

[30] R.D. Allan, H.W. Dickenson, G.A.R. Johnston, R. Kazlauskas, K.N. Mewett, Structural analogues of ZAPA as GABA(a) agonists, Neurochem. Int. 30 (1997) 583–591, https://doi.org/10.1016/S0197-0186(96)00094-0.

[31] F.N. Shirota, J.M. Stevens-Johnk, E.G. DeMaster, H.T. Nagasawa, Novel prodrugs of cyanamide that inhibit aldehyde dehydrogenase in vivo, J. Med. Chem. 40 (1997) 1870–1875, https://doi.org/10.1021/jm9606296.

[32] A. Gładysz-Płaska, M. Majdan, B. Tarasiuk, D. Sternik, E. Grabias, The use of halloysite functionalized with isothiouronium salts as an organic/inorganic hybrid adsorbent for uranium(VI) ions removal, J. Hazard. Mater. 354 (2018) 133–144, https://doi.org/10.1016/j.jhazmat.2018.03.057.

[33] K.A. Venkatesan, B. Robert Selvan, M.P. Antony, T.G. Srinivasan, P.R. Vasudeva Rao, Extraction of palladium from nitric acid medium by commercial resins with phosphinic acid, methylene thiol and isothiouronium moieties attached to polystyrene-divinylbenzene, J. Radioanal. Nucl. Chem. 266 (2005) 431–440, https://doi.org/10.1007/s10967-005-0928-x.

[34] M. Ferreira, L.S. Assunção, A.H. Silva, F.B. Filippin-Monteiro, T.B. Creczynski-Pasa, M.M. Sá, Allylic isothiouronium salts: the discovery of a novel class of thiourea analogues with antitumor activity, Eur. J. Med. Chem. 129 (2017) 151–158, https://doi.org/10.1016/j.ejmech.2017.02.013.

[35] M. Ouyang, J.S. Remy, F.C. Szoka, Controlled template-assisted assembly of plasmid DNA into nanometric particles with high DNA concentration, Bioconjug. Chem. 11 (2000) 104–112, https://doi.org/10.1021/bc990101q.

[36] T.K. Bronich, M. Ouyang, V.A. Kabanov, A. Eisenberg, F.C. Szoka, A.V. Kabanov, Synthesis of vesicles on polymer template, J. Am. Chem. Soc. 124 (2002) 11872–11873, https://doi.org/10.1021/ja020509p.

[37] H.H. Hefni, N.A. Negm, Interactions of glycols with dodecyl isothiouronium cationic surfactant on the surface active parameters, J. Surfactant Deterg. 16 (2013) 751–756, https://doi.org/10.1007/s11743-013-1487-8.

[38] N.A. Negm, A.S. Mohamed, S.M. Ahmed, M.A. El-Raouf, Polymer-cationic surfactant interaction: 1. Surface and physicochemical properties of polyvinyl alcohol (PVA)-S-alkyl isothiouronium bromide surfactant mixed systems, J. Surfactants Deterg. 18 (2015) 245–250, https://doi.org/10.1007/s11743-014-1665-3.

[39] S.T. Keera, N.A. Negm, S.M. Ahmed, A.M. Badawi, Surface parameters and corrosion inhibition of some isothiouranium derivatives, J. Sci. Ind. Res. (India). 61 (2002) 712–718.

[40] G.M. Sheldrick, A short history of SHELX, Acta Crystallogr. Sect. A Found. Crystallogr. 64 (2008) 112–122, https://doi.org/10.1107/S0108767307043930.

[41] L. Krause, R. Herbst-Irmer, G.M. Sheldrick, D. Stalke, Comparison of silver and molybdenum microfocus X-ray sources for single-crystal structure determination, J. Appl. Crystallogr. 48 (2015) 3–10, https://doi.org/10.1107/S1600576714022985.

[42] A. Chatterjee, S.P. Moulik, S.K. Sanyal, B.K. Mishra, P.M. Puri, Thermodynamics of micelle formation of ionic surfactants: a critical assessment for sodium dodecyl sulfate, cetyl pyridinium chloride and dioctyl sulfosuccinate (Na salt) by microcalorimetric, conductometric, and tensiometric measurements, J. Phys. Chem. B 105 (2001) 12823–12831, https://doi.org/10.1021/jp0123029.

[43] A.I. Rusanov, Thermodynamics of ionic micelles, Russ. Chem. Rev. 58 (1989) 101–116, https://doi.org/10.1070/rc1989v058n02abeh003429.

[44] P. Lianos, R. Zana, Fluorescence probe studies of the effect of concentration on the state of aggregation of surfactants in aqueous solution, J. Colloid Interface Sci. 84 (1981) 100–107, https://doi.org/10.1016/0021-9797(81)90263-0.

[45] P.J. Tummino, A. Gafni, Determination of the aggregation number of detergent micelles using steady-state fluorescence quenching, Biophys. J. 64 (1993) 1580–1587, https://doi.org/10.1016/S0006-3495(93)81528-5.

[46] D.H. Wu, A. Chen, C.S. Johnson, An improved diffusion-ordered spectroscopy experiment incorporating bipolar-gradient pulses, J. Magn. Reson. Ser. A 115 (1995) 260–264, https://doi.org/10.1006/jmra.1995.1176.

[47] P. Stilbs, Fourier pulsed-gradient studies of molecular diffusion, Prog. NMR Spectrosc. 19 (1987) 1–45.

[48] O. Söderman, P. Stilbs, W.S. Price, NMR studies of surfactants, Concepts Magn. Reson. Part A Bridg. Educ. Res. 23 (2004) 121–135, https://doi.org/10.1002/cmr.a.20022.

[49] A.D. Voloshina, V.E. Semenov, A.S. Strobykina, N.V. Kulik, E.S. Krylova, V.V. Zobov, V.S. Reznik, Synthesis and antimicrobial and toxic properties of novel 1,3-bis (alkyl)-6-methyluracil derivatives containing 1,2,3- and 1,2,4-triazolium fragments, Russ. J. Bioorganic Chem. 43 (2017) 170–176, https://doi.org/10.1134/S1068162017020170.

[50] R.R. Sharipova, M.G. Belenok, B.F. Garifullin, A.S. Sapunova, A.D. Voloshina, O.V. Andreeva, I.Y. Strobykina, P.V. Skvortsova, Y.F. Zuev, V.E. Kataev, Synthesis and anti-cancer activities of glycosides and glycoconjugates of diterpenoid isosteviol, Medchemcomm. 10 (2019) 1488–1498, https://doi.org/10.1039/c9md00242a.

[51] G.A. Gainanova, G.I. Vagapova, V.V. Syakaev, A.R. Ibragimova, F.G. Valeeva, E.V. Tudriy, I.V. Galkina, O.N. Kataeva, L.Y. Zakharova, S.K. Latypov, A.I. Konovalov, Self-assembling systems based on amphiphilic alkyltriphenylphosphonium bromides: elucidation of the role of head group, J. Colloid Interface Sci. 367 (2012) 327–336, https://doi.org/10.1016/j.jcis.2011.10.074.

[52] J. Łuczak, C. Jungnickel, M. Joskowska, J. Thöming, J. Hupka, Thermodynamics of micellization of imidazolium ionic liquids in aqueous solutions, J. Colloid Interface Sci. 336 (2009) 111–116, https://doi.org/10.1016/j.jcis.2009.03.017.

[53] Y. Yang, B. Yin, Q. Li, U. Englert, (2-Bromoethyl)trimethylammonium bromide and thiourea: A comparative study of three crystal structures, J. Mol. Struct. 920 (2009) 401–408, https://doi.org/10.1016/j.molstruc.2008.11.044.

[54] P. Carpena, J. Aguiar, P. Bernaola-Galván, C. Carnero Ruiz, Problems associated with the treatment of conductivity-concentration data in surfactant solutions: simulations and experiments, Langmuir. 18 (2002) 6054–6058, https://doi.org/10.1021/la025770y.

[55] A.R. Tehrani-Bagha, K. Holmberg, Solubilization of hydrophobic dyes in surfactant solutions, Materials (Basel). 6 (2013) 580–608, https://doi.org/10.3390/ma6020580.

[56] A.B. Mirgorodskaya, R.A. Kushnazarova, S.S. Lukashenko, A.D. Voloshina, O.A. Lenina, L.Y. Zakharova, O.G. Sinyashin, Carbamate-bearing surfactants: Micellization, solubilization, and biological activity, J. Mol. Liq. 269 (2018) 203–210, https://doi.org/10.1016/j.molliq.2018.08.007.

[57] J. van Stam, S. Depaemelaere, F.C. De Schryver, Micellar aggregation numbers - a fluorescence study, J. Chem. Educ. 75 (1998) 93–98, https://doi.org/10.1021/ed075p93.

[58] P. Quagliotto, N. Barbero, C. Barolo, K. Costabello, L. Marchese, S. Coluccia, K. Kalyanasundaram, G. Viscardi, Characterization of monomeric and gemini cationic amphiphilic molecules by fluorescence intensity and anisotropy, Dyes Pigments 82 (2009) 124–129, https://doi.org/10.1016/j.dyepig.2008.12.002.

[59] H. Schott, Solubilization of a water-insoluble dye as a method for determining micellar molecular weights, J. Phys. Chem. 70 (1966) 2966–2973, https://doi.org/10.1021/j100881a041.

[60] Y. Liang, D. Liang, Z. Hu, D. Cao, Synthesis and physicochemical characterization of chiral Pyrrolidinium-based surfactants, J. Dispers. Sci. Technol. 36 (2015) 831–837, https://doi.org/10.1080/01932691.2014.926252.

[61] G.A. Gaynanova, G.I. Vagapova, F.G. Valeeva, E.A. Vasilieva, I.V. Galkina, L.Y. Zakharova, O.G. Sinyashin, A novel supramolecular catalytic system based on amphiphilic triphenylphosphonium bromide for the hydrolysis of phosphorus acid esters, Colloids Surfaces A Physicochem. Eng. Asp. 489 (2016) 95–102, https://doi.org/10.1016/j.colsurfa.2015.10.032.

[62] E.A. Burilova, T.N. Pashirova, S.S. Lukashenko, A.S. Sapunova, A.D. Voloshina, E.P. Zhiltsova, J.R. Campos, E.B. Souto, L.Y. Zakharova, Synthesis, biological evaluation and structure-activity relationships of self-assembled and solubilization properties of amphiphilic quaternary ammonium derivatives of quinuclidine, J. Mol. Liq. 272 (2018) 722–730, https://doi.org/10.1016/j.molliq.2018.10.008.

[63] E.P. Zhiltsova, T.N. Pashirova, R.R. Kashapov, N.K. Gaisin, O.I. Gnezdilov, S.S. Lukashenko, A.D. Voloshina, N.V. Kulik, V.V. Zobov, L.Y. Zakharova, A.I. Konovalov, Alkylated 1,4-diazabicyclo[2.2.2]octanes: self-association, catalytic properties, and biological activity, Russ. Chem. Bull. Int. Ed. 61 (2012) 113–120.

[64] N. Joondan, P. Caumul, M. Akerman, S. Jhaumeer-Laulloo, Synthesis, micellisation and interaction of novel quaternary ammonium compounds derived from L-phenylalanine with 1,2-dipalmitoyl-sn-glycero- 3-phosphocholine as model membrane in relation to their antibacterial activity, and their selectivity over human, Bioorg. Chem. 58 (2015) 117–129, https://doi.org/10.1016/j.bioorg.2015.01.001.

[65] M. Berditsch, S. Afonin, J. Reuster, H. Lux, K. Schkolin, O. Babii, D.S. Radchenko, I. Abdullah, N. William, V. Middel, U. Strähle, A. Nelson, K. Valko, A.S. Ulrich, Supreme activity of gramicidin S against resistant, persistent and biofilm cells of staphylococci and enterococci, Sci. Rep. 9 (2019) 1–15, https://doi.org/10.1038/s41598-019-54212-z.